IEEE Access
Multidisciplinary | Rapid Review | Open Access Journal

Received January 30, 2020, accepted February 9, 2020, date of publication March 2, 2020, date of current version March 31, 2020.

Digital Object Identifier 10.1109/ACCESS.2020.2977396

Grid Map Construction and Terrain Prediction for Quadruped Robot Based on C-Terrain Path

ZHE LI[1], YIBIN LI[1], XUEWEN RONG[1], AND HUI ZHANG[2]
[1]School of Control Science and Engineering, Shandong University, Jinan 250061, China
[2]School of Electrical Engineering and Automation, Qilu University of Technology (Shandong Academy of Sciences), Jinan 250353, China

Corresponding author: Yibin Li (liyb@sdu.edu.cn)

This work was supported in part by the General Program of National Natural Science Foundation of China under Grant U1613223, and in part by the National Key Research and Development Project under Grant 2017YFC0806505 and Grant 2015AA042201.

ABSTRACT In general, grid map based path planning algorithms are employed in the robotics arena. The algorithm uses a grid map to represent environmental information, standardized. Compared with feature maps and topological maps, the algorithm realizes the construction of environmental maps in a more direct way, and has the characteristics of fast, simple and efficient.The integration and prediction of terrain is an unavoidable problem and the traditional raster map prediction method is based on the research of the terrain data itself, and lacks dynamic supplement for the path planning process. When the environmental data changes, the classification algorithm can only be re-executed, and the past data is completely discarded. Since the planned path is unlikely to change, the terrain tends to be stable. To solve this problem, this paper proposes a concept of C(circular)-terrain band following path nodes and terrain construction and prediction methods. The C-Terrain method first obtains an ordered set of passing points at the initial moment, based on the complete path planning. Then an ordered sequence of influence function values is obtained, which depends on the selection of the terrain band and the adjustment of related parameters. Finally, regression methods such as machine learning are used to complete the prediction of the path and location terrain, and the unknown path and terrain are predicted. The experimental results prove the accuracy and practical value of the C-T method.

INDEX TERMS Quadruped robot, path planning, grid map, C-terrain.

I. INTRODUCTION

For quadruped robots, the ability to identify terrain is the key to improving motion efficiency in complex environments. For a conventional wheeled robot or crawler robot, depending on the vision system it is equipped with, the sliding can be prevented and the passable area can be selected [1], [2].

For quadruped robots, in order to improve the stability of their movements, different gaits must be chosen, depending on the terrain. Under different gait, the robot implements different motion control strategies to improve the environment adaptability of the robot. For example, when the robot is in a sandy environment, since the leg joints of the robot are prone to sinking, the strategy of landing and lifting the robot needs to be appropriately changed to reduce the influence of the subsidence on the stability of the robot and improve the stability of the robot.

The associate editor coordinating the review of this manuscript and approving it for publication was Di Zhang.

When the robot is running on a ground with a small friction coefficient, it is necessary to detect, prevent and compensate the sliding of the robot in time. When the robot walks on the gravel ground, the height of the lifting leg of the robot must be adjusted to prevent the robot from falling. Therefore, improving the ability of the robot to recognize the terrain is the key to terrain classification. And the appropriate terrain features need to be extracted, while more efficient terrain classification algorithms need to be selected. This paper focuses on the terrain classification method of robot vision system based on raster map.

In the traditional terrain classification method, there is generally an extraction method based on terrain image color features or image texture features. For the method of image color feature extraction, the local distribution of colors in the image cannot be described. Since the same image has different texture material information, under different lighting and visual conditions. Therefore, the classification method has better classification accuracy and reliability based on image

texture. In the past 30 years, the extraction method based on image texture features has been successfully applied [3], [4].

In the current terrain classification method, the svm method or the neural network method is generally adopted. In the svm method, the initial parameters have a great influence on the performance of the network. The terrain classification method using neural network is accompanied by low computational efficiency and slow convergence speed, which limits the application of this method.

In this paper, the concept of terrain band is proposed and integrated for grid map, and a fast and accurate terrain classification and prediction method is proposed as shown in Figure 1. The terrain classification method proposed in this paper can follow the path nodes. When the local shape changes, the algorithm uses incremental operations to improve computational efficiency and reacts the overall terrain of the path in new forms, while unknown terrain can be predicted.

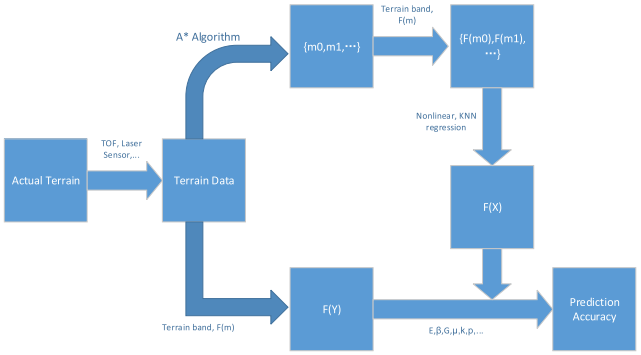

FIGURE 1. Terrain prediction based on C-terrain path.

II. MAP CLASSIFICATION METHOD AND TERRAIN BAND

In the field of robotics, compared with feature maps and topological maps, raster maps enable the construction of environmental maps in a more direct way, with fast, simple and efficient features [5]. When faced with robot path planning problems, it is inevitable to classify the raster maps to make it easier and more accurate to judge the passability of the grid nodes.

Based on topographic data, the traditional raster map classification method is used for mining analysis. The algorithm lacks dynamic supplement for the path planning process.

When the environmental data changes, the traditional terrain classification method can only re-execute the algorithm operation, and completely abandon the historical data during the operation. However, in the actual process, the planned path is unlikely to change stepwise, and the terrain itself is usually relatively stable [6], [7]. In response to this problem, this paper proposes the concept of terrain bands following path nodes.

The terrain band can reflect the passability of the path. Based on this concept, the terrain classification method proposed in this paper is based on the completed path planning, and classifies the terrain for the existing path. This ensures that when the environment map changes rapidly, the algorithm can provide more accurate terrain information for more important path points because the path offset is not large.

Moravecc [8] proposed to discretize the height direction based on the plane grid to realize the three-dimensional grid map. Carsten *et al.* [9] used a similar raster map in the study of their path planning algorithms. Fong, Gutmann, LiuHhuajun Patrick Pfaff et al. based on a two-dimensional grid map, the maximum height or average height of the terrain in each grid is stored to construct an elevation map, an extended elevation map or a layered map [10]–[12]. This not only can achieve the performance of the three-dimensional raster map, but also reduce the amount of raster map data.

A* algorithm is a common grid map path planning method, which was proposed by Nilsson in 1980. It can search the optimal path to target point by contrast evaluation function. The core of it is to add heuristic search part based on Dijkstra algorithm. Its evaluation function is

$$f(n) = g(n) + h(n) \tag{1}$$

$f(n)$ is the evaluation function, $g(n)$ represents the path cost from the initial point n to any node. $h(n)$ said heuristic evaluation price, from the node n to the target point.

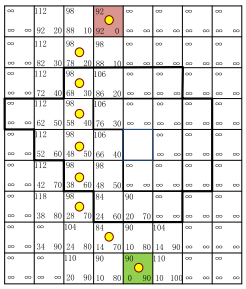

FIGURE 2. Equipotential line in grid map.

As shown in Figure 2, for each grid, the value of $g(n)$ is marked in the lower left corner, the value of $h(n)$ is marked in the lower right corner, and the value of $f(n)$ is marked in the upper left corner. Green node is the starting node, red is the target node, and yellow point is the pathway node. Bold lines indicate contour lines, obtained by TOF cameras or laser sensors. The equipotential line in the traditional map or the medium potential surface of the force field can quickly and effectively complete the classification of the topographic points. At the same time, by comparing the equipotential lines and equipotential surfaces of any two points, the topography difference can be quickly calculated. These concepts are essentially the discretization of linear maps, which coincides with the original intention of grid map design.

Based on this concept, the equipotential surface is introduced into the grid map, and in order to accurately reflect the passability information of the path, the terrain strip is followed by the path node. This form of terrain representation can follow the path nodes and reflect the surrounding

equipotential surface information, which is the terrain band proposed in this paper.

Based on the classification method of the terrain band, the terrain data corresponds to the path point. When the local shape changes, it is easy to find the influence of the change point on the path. The algorithm can intuitively indicate the difficulty of passing the terrain of different planning paths. This terrain classification method for the overall path provides a new passability assessment criterion for path planning.

III. C-TERRAIN SELECTION

The terrain classification method proposed in this paper is based on the terrain band. Traditional raster maps are stored in the form of data columns, but the C-terrain method stores the raster map as a data strip C(n) that follows the path node.

$$C(n) = \{F(m_1), F(m_2), \ldots, F(m_n)\} \tag{2}$$

where $\{m_n\}$ is the set of path nodes obtained by the A* algorithm at the initial moment, m_1 is the starting point, and m_n is the target point. F(m) is the influence function value of the terrain band corresponding to node m. And this benefits from the terrain band and the different selection methods of the terrain band determine the different focuses of the constructed map.

There are many ways to choose the terrain band. Different selection methods can more accurately reflect the shape or undulation of the surrounding terrain. The concept of equipotential surface is borrowed to make the terrain band more accurately reflect the terrain shape. This selection method is in line with the physical meaning of the terrain band. An arbitrary point contained in a terrain band has the same height difference as the corresponding passing node. The height value of the node is obtained by a TOF camera or a laser sensor. Or the algorithm selects the nodes contained in the terrain band in a circular (rectangular) manner. This method focuses on reflecting the terrain undulation around the nodes. Because the shape of the terrain band is fixed, the algorithm is simple and fast, which is also beneficial to be combined with path planning. The height value of the passing point is regarded as the ground potential, which is used as a reference by the algorithm.

Two different selection methods are now compared. When planning the path of the grid map, the A* algorithm and its derivative algorithm are used to form the initial path, that is, the initial path node set $\{m_n\}$. Select path points m_0,m_1,m_2, ... in order of path, for any path point. Then the gradient base E of the terrain band and the gradient coefficients $\alpha = 0, 1, 2 \ldots$ were set to divide the terrain nodes into distinct categories. E is manually selected based on the height information obtained by a TOF camera or laser sensor.

when $\alpha = 0$, only the current grid is considered.

when $\alpha = 1$, all grids have a gradient difference E, compared to the current node.

when $\alpha = 2$, all grids have a gradient difference 2E.

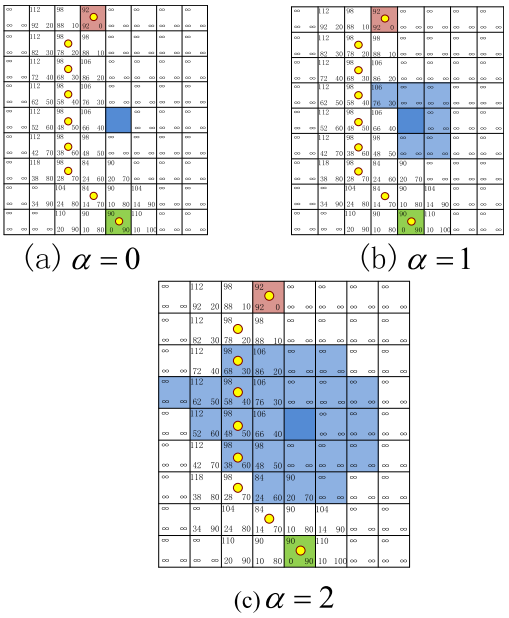

FIGURE 3. C-terrain band with equal height difference.

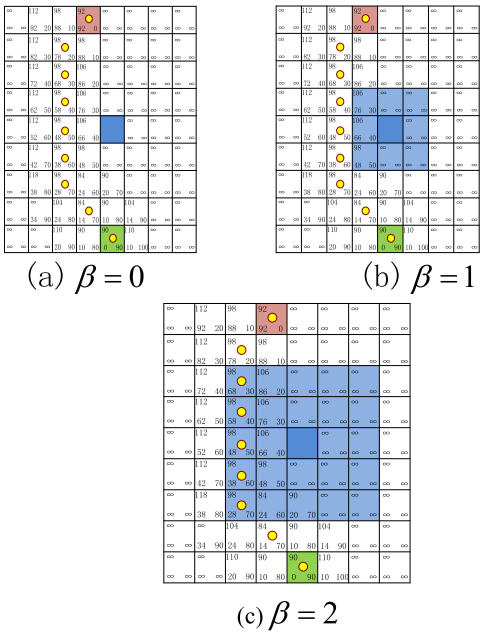

FIGURE 4. C-terrain band with equal distance difference.

The breadth coverage factor of terrain β is set to $\beta = 0, 1, 2,$

$\beta = 0$ indicates only the current grid is considered.

$\beta = 1$ indicates the 8 grids around the current node.

$\beta = 2$ indicates the 24 grids.

β is added to the algorithm as an adjustable global parameter, and all nodes use the same β-value. A higher β-value can reflect the characteristics of the terrain band more widely. At the same time, too high β-value is easy to cause overfitting, and it will also increase the amount of calculations

needlessly. In general, the value of β is preferably between 2 and 4, which is also related to the selection of the point cloud when the grid map is constructed and the zoom ratio when the Quadruped Robot is equivalent to a mass point.

When α, β takes 3 or other values, the result can be calculated by analogy. Regardless of the terrain selection method used, the follow-up of the path points can be implemented, using the calculation results of the influence function. However, the terrain bands acquired by the first method are usually irregular patterns. In the process of path planning based on raster maps, moving entities such as robots are often equivalent to nodes by proportional scaling. For different terrain such as sand, brick, and steps, the size and height of the map will change, and the value of E must change accordingly. The fixed E value cannot effectively classify different kinds of terrain nodes. At the same time, considering that the grid map will be frequently zoomed in the path planning and practical application process, this paper takes the second terrain band selection method. This is one of the reasons for replacing circles with rectangles.

IV. INFLUENCE FUNCTION AND C-TERRAIN PATH CONSTRUCTION

Since the second terrain band selection method is selected, the influence function needs to reflect the mean value of the ground potential difference of the surrounding nodes. The distance average can use Manhattan distance, or Euclidean distance, or even cosine distance.

Different distance measurement methods are applied, which has a great impact on the final result. In general, raster map data collections have many features. But if the Euclidean distances between any two nodes are equal, there is no way to compare them by Euclidean distance.

If the Manhattan distance is used, the algorithm will have higher stability. However, if some of the feature values in the terrain data set are large, the distance relationship between other feature points will be masked. Finally, the cosine distance is suitable for use when the feature vector is large. But it discards valuable information such as vector length, and it has a larger amount of computation.

When the Euler distance is used, the terrain strip is selected to be selected, which is more realistic. But many path planning algorithms use Manhattan distance. To ensure consistency between the data, set the influence function as follows,

$$F(m_1) = \frac{\sum f(m_1, m_2)}{n(m_1)} = \frac{\sum G(m_1)\frac{|dm_1 - dm_2|}{dx+dy}}{n(m_1)} \tag{3}$$

$n(m_2)$ represents the nodes amount on the certain circle, $|dm_1 - dm_2|$ represents the elevation difference between the two points, dx,dy represents the Manhattan distance, and $G(m_1)$ represents the influence coefficient of the path node type to which m1 belongs. When $\beta > 2$, the influence factor of dm_2 drops rapidly. Its impact will be ignored in order to simplify the calculation.

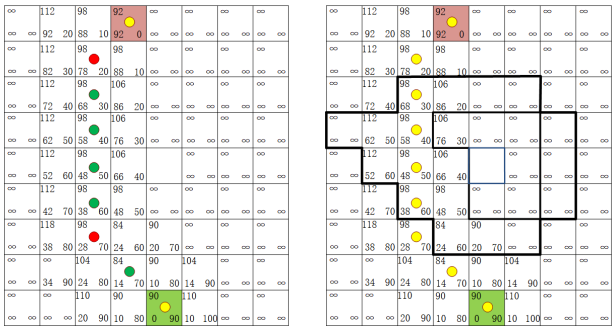

FIGURE 5. Inflection point and equipotential line.

The value of G is related to the position of $|m_t|$ in the set of path points.

$$\begin{cases} G(m_t) > 1, & m_t \in C \\ G(m_t) = 1, & m_t \in \{m_0, m_n\} \\ G(m_t) < 1, & \text{else} \end{cases} \tag{4}$$

where C is the set of all inflection points of the path. As shown in Figure 5, when the current node is an inflection point (red point), the node point will keep a higher G value to provide a more sensitive topographic response, compared to when it belongs to a straight line. The G-value of the inflection point is set higher to distinguish it from the passing point of the straight portion. Increasing the value of the influence function artificially is to set obvious characteristics of the data sequence in order to predict the inflection point of the path in the unknown terrain.

In the process of map construction, the algorithm first completes the path planning at the initial moment by A* and its derivative algorithm at the initial moment. After the initial path node set is obtained, the algorithm selects the terrain band. For the nodes in the set, the influence function is used to obtain the terrain passing coefficient of each node, and finally the passing coefficient set of the terrain band is obtained, which follows the initial path node.

The following compares the traditional method with the representation of the following path points. For traditional methods, if the first method is adopted, nodes with similar elevations in the terrain data will be divided into several sets. Essentially it is to increase the raster map equipotential line. In the path planning process, although it is possible to use the equipotential line to achieve the prediction of the passing difficulty, the algorithm cannot quickly and effectively evaluate the overall passing difficulty of the current path, and the storage space cannot be optimized.

If the terrain of all nodes is fully considered, the amount of calculation will be large, with accurate terrain information. In this algorithm, the time coefficient is introduced to achieve the algorithm within the specified time limit. At the same time, new passability assessment criteria are provided.

The terrain-based algorithm focuses on the overall terrain of the path, and these nodes are all passable regions in

the initial sense. The value of the topographical coefficient reflects the cost of adoption. Based on this coefficient and the barrier performance of the robot, the raster map can be classified.

V. TERRAIN PREDICTION BASED ON C-TERRAIN PATH

Unknown terrain can be predicted using known terrain information. In order to simplify the calculation, the terrain strips corresponding to the nodes are selected in reverse order and form a set, from the end of the path. The selection of nodes is related to the number of inflection points and the length of the internodes. Then the nonlinear regression fitting curve is performed. Since a finite number of adjacent nodes are selected, the graph is close to the parabolic shape, so it can be predicted by the quadratic curve model of nonlinear regression. Establish a predictive mode nonlinear regression quadratic curve model as,

$$y_i = \beta_1 + \beta_2 x_i + \beta_3 x_i^2 + \in_i \tag{5}$$

let $x_i^2 = x_i'$,

$$y_i = \beta_1 + \beta_2 x_i + \beta_3 x_i^{'} + \in_i \tag{6}$$

The matrix form of the above formula is $Y = XB + \in$. The least squares method is then used for parameter estimation, and the residual is set to E between the observed value and the model estimate. then $E = Y - \hat{Y}$, $\hat{Y} = XB$, According to the least square method, $E'E = (Y - \hat{Y})'(Y - \hat{Y})$, the following formula is obtained

$$E'E = (Y - \mathrm{XB})'(Y - \mathrm{XB}) \tag{7}$$

From the extremum principle and the matrix derivation method, we derive the B and make it equal to zero.

$$\frac{\partial E'E}{\partial B} = \frac{\partial (Y - XB)'(Y - XB)}{\partial B} = \frac{\partial (Y'Y - 2Y'XB + B'X'XB)}{\partial B} \tag{8}$$

In summary, the estimated value of the regression coefficient vector B is, $\widehat{B} = (X'X)^{-1}(X'Y)$. The most commonly used tests in quadratic regression are the R test and the F test,

$$R = \sqrt{1 - \frac{\sum (y_i - \hat{y})^2}{\sum (y_i - \bar{y})^2}}, \quad F = \frac{R^2}{1 - R^2}(n - 3)/2 \tag{9}$$

Now predict the terrain information of the unknown area according to the prediction model, according to the above formula $X'X, X'Y, \widehat{B} = (X'X)^1(X'Y)$ and,

$$\hat{y}_\mathrm{i} = \hat{\beta}_1 + \hat{\beta}_2 x_i + \hat{\beta}_3 x_i^2 \tag{10}$$

$$\mathrm{R} = \sqrt{1 - \frac{\sum \mathrm{y}_\mathrm{i}^2 - \hat{\beta}_1 \sum y_i - \hat{\beta}_2 \sum x_i y_i - \hat{\beta}_3 \sum x_i' y_i}{\sum y_i^2 - n\bar{y}^2}} \tag{11}$$

$$S = \sqrt{\frac{\sum (y_i - \hat{y}_i)^2}{n - 3}} \tag{12}$$

S is the estimated standard error.

Considering the actual operation process, it is necessary to obtain the suboptimal solution in a limited time, so the time factor ε is introduced and the number of inflection points and the internode length are considered. And the prediction time is limited to a limited time T to prevent the response time of the algorithm from being too long, so as to maintain the efficiency of the algorithm. On the one hand, because the algorithm sets β, G,k and other global parameters that need to be adjusted manually and the size of the input terrain data is different, inappropriate parameter values will often cause the algorithm to consume a lot of time. On the other hand, sub-optimal solutions obtained by setting time parameter limits are often more suitable for practical problems.

There are many ways to adjust the algorithm operation time. This article uses increasing μ to change the weight of h(n) in the heuristic part of the A* algorithm. This will change the judgment of the path calculation planning method for the node's passability and the cost of passing, thereby changing the set of nodes that change the path. Usually smaller μ will have longer time consuming and more accurate and complicated path results, while larger μ corresponds to shorter time consuming and flat path.

$$f(n) = g(n) + \mu \cdot h(n) \tag{13}$$

The constraints of the node are as follows. $|N(n) - N(n-1)| > \mathrm{Q}$, any two adjacent nodes may not be too close, otherwise one of them will be discarded. $|N(g) - N(0)| < \varepsilon \mathrm{R}$, the finite number of nodes are selected in reverse order, and the expansion factor ε is introduced. The value is decremented from 1 until the operation time is within T. When $N_{s\max} = 0, 1$, the inflection points number of the path is 0 or 1, all path nodes are included in the research content. Otherwise $N_{s\max} \geq 2$, the node before the second inflection point is included in the study.

Although the non-linear regression prediction method can obtain topographic prediction information, it has limitations on the data characteristics of the sample. This paper uses the python-based SKlearn module to perform regression processing on terrain data. Using Sklearn's regression module algorithm, vector regression (SVR), ridge regression, Lasso regression, elastic network (Elastic Net), minimum angle regression (LARS), Bayesian regression, and various robust regression algorithms can be implemented. All algorithms use the Boston House Price dataset, where the independent variables are numeric. K-Nearest Neighbors (or KNN) determines K similar instances for new data instances and uses the mean or median as the predicted values, which is suitable for the prediction of terrain bands in this paper.

The number of nearest algorithm samples can be a custom constant or follow the density of the data points. It should be noted that, unlike the Manhattan distance used in this paper, the measure of the distance is the Minkowski distance, so the corresponding conversion is required. The definition of Minkowski distance is as follows. When p = 2, it is the

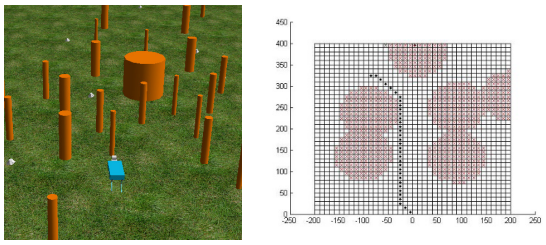

FIGURE 6. Simulation environment with Webots and Matlab.

Euclidean distance, and p = 1 means the Manhattan distance.

$$M = \left(\sum_{i=1}^{n} |x_i - y_i|^p\right)^{1/p}$$
$$P = (x_1, x_2, x_3, \ldots, x_n), \quad Q = (y_1, y_2, y_3, \ldots, y_n) \in R^n \quad (14)$$

The Minkowski distance provides a parameter p to quickly switch between Euclidean distance, Manhattan distance, etc. Different distance standards can be applied to the C-T algorithm. Considering the compatibility with the A* algorithm, Manhattan distance is used as the standard.

The Neighbors-based method is called a non-generalizing machine learning method because the algorithm simply ''remembers'' all training data and converts it into a fast index structure such as a sphere tree or a KD tree. The Knn algorithm has successfully solved classification and regression problems including handwritten digits and satellite imagery. As a non-parametric method, it is suitable for classification problems with irregular boundaries. It should be noted that instead of using the knn algorithm for data classification, the nearest neighbor idea is used for regression prediction.

Different k values correspond to different prediction accuracy and time consumption. The knn terrain classification algorithm has a coincidence with the idea of the terrain band, and the selection of the k-value is similar to the bandwidth of the terrain band. The knn algorithm does not have actual physical meaning, and the terrain algorithm is easy to acquire and separate terrain data. It is one of the future research contents to compare the classification of terrain with the idea of terrain with the most advanced thought.

VI. SIMULATION AND EXPERIMENT

In order to evaluate the performance of the related algorithms mentioned in this paper, the algorithm was tested in Webots, Matlab and Python platform respectively. The simulation environment is shown in the Figure 6. The simulation in Matlab is convenient for theoretically testing the accuracy and feasibility of the algorithm. And the simulation in Webots involves system errors such as multi-sensor fusion and attitude response delay, which is closer to the actual situation of the quadruped robot platform.

In order to test the planning efficiency based on terrain terrain classification, this section compares the number of required rasters and the total number of grids between the original method and the terrain-based terrain classification method, in the same terrain environment.

TABLE 1. Path length and time cost based on A* and C-terrain.

Num	Total Length/m		Time Cost/s	
	A*	C-T	A*	C-T
1	20.97	20.95	76.55	82.04
2	15.87	15.82	57.97	60.94
3	17.19	17.04	59.85	63.27
4	20.27	20.17	61.63	63.56
5	17.82	17.97	60.45	62.58
6	11.17	10.80	48.24	51.74
7	18.73	18.15	58.58	60.05
8	18.75	18.39	59.77	60.84
9	15.41	14.92	56.65	57.42
10	13.57	12.91	52.69	54.03

TABLE 2. Total number of grids searched by A* and C-t.

Num	Amount of grids		A*/C-T
	A*	C-T	
1	32405	4767	6.80
2	30710	3718	8.26
3	34001	3477	9.78
4	45839	7805	5.87
5	39813	4930	8.08
6	35892	3725	9.64
7	23372	3699	6.32
8	27200	3292	8.26
9	18140	2954	6.14
10	32403	3711	8.73

When the local shape changes dynamically, the terrain-based classification method is easy to find the influence of the changing nodes on the path, because the terrain data corresponds to the path points.

As shown in Figure 7 above, the blue data indicates the total length of the planned path of the A* algorithm, the time consumption and the number of traversed grids. The red data represents the length of the C-terrain algorithm planning path, the time consumption and the amount of traversal grids. The comparative analysis shows that although the path length of A* is almost the same as that of the C-terrain, the number of traversal grids of C-terrain algorithm is obviously smaller

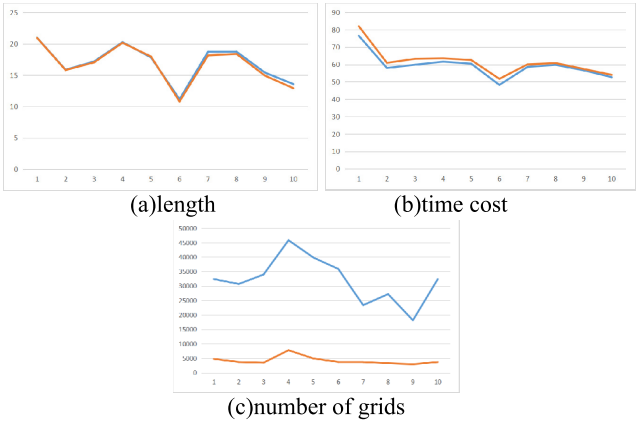

FIGURE 7. Effectiveness comparison between A* and C-t.

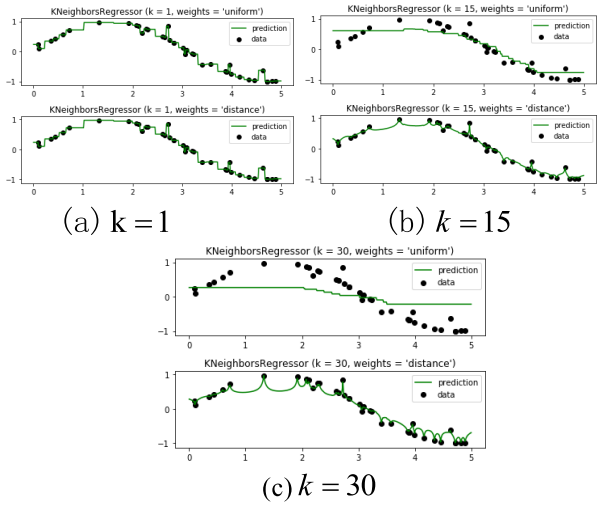

FIGURE 8. KNN prediction based on different k value.

than that of A* algorithm, and the extra time consumption is not significant. If we consider only traversing the grid number, the C-terrain algorithm has more than 6 times the search efficiency of the A* algorithm.

The change of the environment map information can be considered as a window shift. The algorithm first compares the current time and the set of path nodes with the previous time, and obtains it through the path planning algorithm. Then discard the nodes that are not in the window and add new nodes, in the order of the nodes. On the basis of the new set of path nodes, the construction of the terrain set is completed.

As can be seen from the Figure 8, the selection of k-value has a great influence on the knn regression prediction algorithm. When the appropriate k-value is chosen, the results of the two algorithms are similar.

The terrain prediction platform was built and simulated for prediction in the Python platform. Comparing the results with the nonlinear regression method, the knn regression algorithm of machine learning has lower requirements on the characteristics of the data set. Although it takes longer,

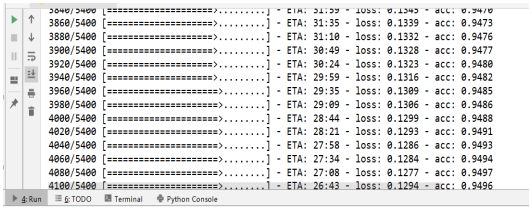

FIGURE 9. The Prediction Accuracy based on C-terrain with python.

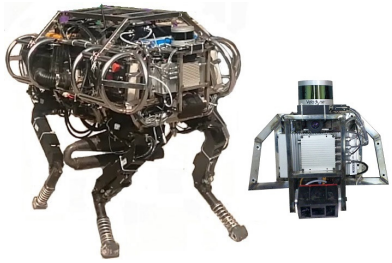

FIGURE 10. Scalf II platform and visual system.

TABLE 3. Prediction accuracy based on nonlinear regression and KNN regression.

NUM	NONLINEAR REGRESSION		KNN REGRESSION		
	QUADRATIC	CUBIC	K=1	K=15	K=30
1	0.79	0.83	0.86	0.92	0.87
2	0.75	0.76	0.91	0.93	0.79
3	0.85	0.86	0.87	0.94	0.81
4	0.81	0.80	0.86	0.90	0.83
5	0.68	0.72	0.88	0.91	0.86
6	0.71	0.81	0.91	0.96	0.87
7	0.82	0.86	0.94	0.95	0.91
8	0.84	0.87	0.87	0.94	0.93
9	0.81	0.79	0.85	0.94	0.87
10	0.74	0.86	0.90	0.89	0.90

the algorithm usually obtains reasonable predictions of terrain results as long as sufficient training samples are provided. Simulations results from Figure 9 show that the algorithm already has enough precision when dealing with relevant map information.

The actual test was performed on the ScalfII platform as shown in Figure 10. The platform uses a VLP-16 3D laser scanner, a GT1910c monocular camera and a SR4500 TOF camera to form its vision system. ScalfII was driven and tested ten times in the environment of stone steps, sand, brick, grass, etc. Each group collected 50,000 frames of data, and each frame was a point cloud composed of 25344 data points. The first 45,000 frames are used for training, and the last

5,000 frames are used as actual data to compare with prediction results and calculate prediction accuracy. It can be known from Table 3 that the KNN regression method has higher stability and maintains higher accuracy while the prediction accuracy does not fluctuate much, compared with the nonlinear regression method. The appropriate K value has a decisive effect on the prediction accuracy under some conditions. In general, the experimental results are basically consistent with the simulation results under the Python platform.

VII. CONCLUSION AND PROSPECT

Based on the concept of equidistant terrain, this paper proposes a method to judge the topographic features of grid nodes based on the characteristics of C-terrain. On this basis, the terrain band is combined with the initial path to form a sequenced set of terrains following the path point. Compared with the original raster terrain processing algorithm, the C-terrain based algorithm is more suitable for actual operation and has more hilarious assimilation processing ability for complex terrain. At the same time, the method of logistic regression and KNN machine learning is used to realize the prediction of unknown terrain. The experiment proves the advantages of C-terrain based map construction method and the accuracy of terrain prediction. This article involves a number of global parameters, β, E, G,p,k, etc. Algorithm performance comparison under different parameter configurations is one of the future research directions. Compared with the traditional algorithm, the proposed C-terrain based algorithm has higher processing performance and stability, especially in the process of processing dynamic terrain information. And the new processing result is optimized based on the initial result, which greatly shortens the time consumption and improves the computational efficiency of the algorithm as a whole.

Obstacle avoidance is an inevitable problem, wherever path planning issues are involved. Obstacle avoidance based on the C-Terrain method is one of the future research focuses. The related evaluation function of each path node in the paper can only reflect the surrounding terrain's passability, and the rough terrain corresponds to the lower tolerance of obstacle terrain. In order to avoid obstacles in the path based on the C-Terrain method, we consider adding a parameter p to reflect the direction of the obstacles. After p forms a sequence according to the C-T method, the p can be predicted, and the path can be shifted according to the fluctuation of p-value to avoid obstacles.

The desired algorithm needs to have efficient computational efficiency in complex environments. The algorithm can obtain as accurate terrain information as possible within the allowed time. For dynamic maps, this paper proposes C-terrain based classification and prediction algorithm, and Euler distance is used to measure grid maps. The incremental terrain processing idea of the algorithm and the method of reducing the computational complexity and increasing the integrity by following the nodes can be applied to other forms of terrain prediction. The next step is to expand the application of the algorithm under other forms of maps. When the local shape information is more complex and the high frequency changes, its dynamic adaptability will face challenges. The next step will be to increase the adaptability of the high frequency map to make it more responsive to actual operational requirements.

REFERENCES

[1] A. Angelova, L. Matthies, D. Helmick, and P. Perona, "Slip prediction using visual information," *Robot., Sci. Syst.*, 2006.

[2] A. Angelova, L. Matthies, D. Helmick, G. Sibley, and P. Perona, "Learning to predict slip for ground robots," in *Proc. IEEE Int. Conf. Robot. Automat. (ICRA)*, May 2006, pp. 3324–3331.

[3] S. Lazebnik, C. Schmid, and J. Ponce, "Beyond bags of features: Spatial pyramid matching for recognizing natural scene categories," in *Proc. IEEE Comput. Soc. Conf. Comput. Vis. Pattern Recognit. (CVPR)*, vol. 2, Jun. 2006, pp. 2169–2178.

[4] Y. Su, D. Tao, X. Li, and X. Gao, "Texture representation in AAM using Gabor wavelet and local binary patterns," in *Proc. IEEE Int. Conf. Syst., Man Cybern.*, Oct. 2009, pp. 3274–3279.

[5] M. W. M. G. Dissanayake, P. Newman, S. Clark, H. F. Durrant-Whyte, and M. Csorba, "A solution to the simultaneous localization and map building (SLAM) problem," *IEEE Trans. Robot. Autom.*, vol. 17, no. 3, pp. 229–241, Jun. 2001.

[6] C. Alan, "Continuous localization using evidence grids," in *Proc. IEEE Int. Conf. Robot. Automat.*, May 1998, pp. 2833–2839.

[7] [Online]. Available: http://cmp.felk.cvut.cz/demos/Omni/mobil/

[8] H. P. Moravec, "Robot spatial perception by stereoscopic vision and 3D evidence grids," CMU Robot. Inst., Pittsburgh, PA, USA, Tech. Rep. CMU-RI-TR-96-34, 1996.

[9] J. Carsten, D. Ferguson, and A. Stentz, "3D field D: Improved path planning and replanning in three dimensions," in *Proc. IEEE/RSJ Int. Conf. Intell. Robots Syst.*, Oct. 2006, pp. 3381–3386.

[10] E. H. L. Fong, W. Adams, F. L. Crabbe, and A. C. Schultz, "Representing a 3-D environment with a 21/2-D map structure," in *Proc. IEEE/RSJ Int. Conf. Intell. Robots Syst. (IROS)*, Oct. 2003, pp. 2986–2991.

[11] J.-S. Gutmann, M. Fukuchi, and M. Fujita, "A floor and obstacle height map for 3D navigation of a humanoid robot," in *Proc. IEEE Int. Conf. Robot. Automat.*, Apr. 2005, pp. 1066–1071.

[12] L. Huajun, Y. Jingyu, and Z. Chunxia, "A generic approach to rugged terrain analysis based on fuzzy inference," in *Proc. Int. Conf. Control, Automat., Robot. Vis. (ICARCV)*, 2004, pp. 1108–1113.

[13] M. Likhachev, G. J. Gordon, and S. Thrun, "ARA*: Anytime A* with provable bounds on sub-optimality," in *Advances in Neural Information Processing Systems*. Cambridge, MA, USA: MIT Press, 2003, pp. 52–89.

[14] A. Stentz, "Optimal and efficient path planning for partially-known environments," in *Proc. IEEE Int. Conf. Robot. Automat.*, May 1994, pp. 3310–3317.

[15] A. Stentz, "The focussed D* algorithm for real-time replanning," in *Proc. Int. Joint Conf. Artif. Intell.*, 1995, pp. 1652–1659.

[16] S. Koenig and M. Likhachev, "Fast replanning for navigation in unknown terrain," *IEEE Trans. Robot.*, vol. 21, no. 3, pp. 354–363, May 2005.

[17] S. Koenig, M. Likhachev, and D. Furcy, "Lifelong planning A*," *Artif. Intell. J.*, vol. 155, nos. 1–2, pp. 93–146, 2003.

[18] C. D. Boor, *A Practical Guide to Splines*. Springer-Verlag, 1978.

[19] P. Dierckx, *Curve and Surface Fitting With Splines*. New York, NY, USA: Clarendon Press, 1995, pp. 63–80.

[20] A. Piazzi and A. Visioli, "Global minimum-jerk trajectory planning of robot manipulators," *IEEE Trans. Ind. Electron.*, vol. 47, no. 1, pp. 140–149, Feb. 2000.

[21] P. Fankhauser, M. Bjelonic, C. D. Bellicoso, T. Miki, and M. Hutter, "Robust rough-terrain locomotion with a quadrupedal robot," in *Proc. IEEE Int. Conf. Robot. Automat. (ICRA)*, May 2018, pp. 1–8.

[22] G. Song and N. Amato, "Randomized motion planning for car-like robots with C-PRM," in *Proc. IEEE/RSJ Int. Conf. Intell. Robots Syst.*, Maui, HI, USA, Oct./Nov. 2001, pp. 37–42.

[23] K. Kim, K. Ko, W. Kim, S. Yu, and C. Han, "Performance comparison between neural network and SVM for terrain classification of legged robot," in *Proc. SICE Annu. Conf.*, 2010, pp. 1343–1348.

[24] C. Semini, V. Barasuol, J. Goldsmith, M. Frigerio, M. Focchi, Y. Gao, and D. G. Caldwell, "Design of the hydraulically actuated, torque-controlled quadruped robot HyQ2Max," *IEEE/ASME Trans. Mechatronics*, vol. 22, no. 2, pp. 635–646, Apr. 2017.
[25] L. Liu, P. Fieguth, G. Kuang, and H. Zha, "Sorted random projections for robust texture classification," in *Proc. Int. Conf. Comput. Vis.*, Nov. 2011, pp. 391–398.
[26] L. Zhe, L. Yibin, R. Xuewen, and Z. Hui, "Path planning based on ADFA* algorithm for quadruped robot," *IEEE Access*, vol. 7, pp. 111095–111101, 2019.
[27] R. Buchanan, T. Bandyopadhyay, M. Bjelonic, and L. Wellhausen, "Walking posture adaptation for legged robot navigation in confined spaces," *IEEE Robot. Automat. Lett.*, vol. 4, no. 2, pp. 2148–2155, Feb. 2019.
[28] A. Elfes, R. Steindl, F. Talbot, F. Kendoul, P. Sikka, T. Lowe, N. Kottege, M. Bjelonic, R. Dungavell, T. Bandyopadhyay, M. Hoerger, B. Tam, and D. Rytz, "The multilegged autonomous eXplorer (MAX)," in *Proc. IEEE Int. Conf. Robot. Automat. (ICRA)*, May 2017, pp. 1050–1057.
[29] M. Bjelonic, T. Homberger, N. Kottege, P. Borges, M. Chli, and P. Beckerle, "Autonomous navigation of hexapod robots with vision-based controller adaptation," in *Proc. IEEE Int. Conf. Robot. Automat. (ICRA)*, May 2017, pp. 5561–5568.
[30] A. Short and T. Bandyopadhyay, "Legged motion planning in complex three-dimensional environments," *IEEE Robot. Autom. Lett.*, vol. 3, no. 1, pp. 29–36, Jan. 2018.

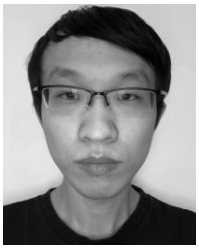

ZHE LI received the bachelor's and master's degrees from the Shandong University of Science and Technology, China, in 2012 and 2014, respectively. He is currently pursuing the Ph.D. degree with the School of Control Science and Engineering, Shandong University, China. His research interests include the environmental perception and path planning for quadruped robot.

YIBIN LI received the bachelor's degree from Tianjin University, China, in 1982, the master's degree from the Shandong University of Science and Technology, China, in 1988, and the Ph.D. degree from Tianjin University, in 2006. He is currently a Professor and an Associate Dean of the School of Control Science and Engineering, Shandong University, China. His research interests include robotics, mechatronics, intelligent control, intelligent vehicles, and so on.

XUEWEN RONG received the bachelor's and master's degrees from the Shandong University of Science and Technology, China, in 1996 and 1999, respectively. He is currently pursuing the Ph.D. degree with the School of Control Science and Engineering, Shandong University, China. He is also a Senior Engineer with the School of Control Science and Engineering, Shandong University, China. His research interests include robotics, mechatronics, hydraulic servo driving technology, and so on.

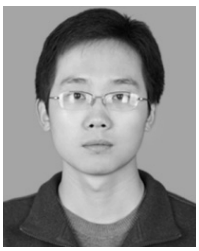

HUI ZHANG received the bachelor's and master's degrees from Shandong Agricultural University, China, in 2009 and 2012, respectively, and the Ph.D. degree from Shandong University, China, in 2016. He is currently a Lecturer with the School of Electrical Engineering and Automation, Qilu University of Technology (Shandong Academy of Sciences), China. His research interests include the environmental perception and path planning for quadruped robot.